Brazilian Journal
of Chemical
Engineering

ISSN 0104-6632
Printed in Brazil
www.abeq.org.br/bjche

Vol. 33, No. 02, pp. 319 - 332, April - June, 2016
dx.doi.org/10.1590/0104-6632.20160332s20140237

DOLOMITE DESULFURIZATION BEHAVIOR IN A BUBBLING FLUIDIZED BED PILOT PLANT FOR HIGH ASH COAL

G. M. F. Gomes[1,2*], C. Philipssen[3], E. K. Bard[1] and G. Souza[1]

[1]Fundação de Ciência e Tecnologia do Estado do Rio Grande do Sul, (CIENTEC), Av. das Indústrias 2277, Distrito Industrial, Laboratory of Combustion, Cachoeirinha - RS, Brasil.
[2]Universidade do Vale do Rio dos Sinos, (UNISINOS), Av. Unisinos 950, Cristo Rei, Department of Engineering, São Leopoldo - RS, Brasil.
[3]Programa de Pós-Graduação em Engenharia de Minas, Metalúrgica e Materiais, Universidade Federal do Rio Grande do Sul, (UFRGS), Av. Bento Gonçalves 9500, Setor 6, Centro de Tecnologia, Laboratório de Siderurgia, Sala 222, Porto Alegre - RS, Brasil.
Phone: + 55 (51) 34396351; Fax: + 55 (51) 33087116
E-mail: gabriel-gomes@cientec.rs.gov.br; gmfae@unisinos.br

(Submitted: December 18, 2014 ; Revised: April 15, 2015 ; Accepted: May 15, 2015)

Abstract - Although fluidized bed *in situ* desulphurization from coal combustion has been widely studied, there are aspects that remain under investigation. Additionally, few publications address Brazilian coal desulphurization via fluidized beds. This study used a 250 kWth bubbling fluidized bed pilot plant to analyze different aspects of the dolomite desulphurization of two Brazilian coals. Superficial velocities of 0.38 and 0.46 m/s, flue gas recycling, Ca/S molar ratios and elutriation were assessed. Results confirmed the influence of the Ca/S molar ratio and superficial velocity – SO_2 conversion up to 60.5% was achieved for one coal type, and 70.9% was achieved for the other type. A recycling ratio of 54.6% could increase SO_2 conversion up to 86.1%. Elutriation and collection of ashes and Ca-containing products did not present the same behavior because a lower wt. % of CaO was collected by the gas controlled mechanism compared to the ash.
Keywords: Fluidized bed; Coal; Desulphurization.

INTRODUCTION

Fluidized bed coal combustion has the advantage of creating SO_2 treatment through a sulphation reaction from the *in situ* injection of dolomite or limestone. This procedure has been widely explored; however, some details and local behaviors based on coal characteristics are still under investigation. Moreover, it should be noted that there is a lack of information concerning Brazilian coal in fluidized beds. Furthermore, according to Anthony and Granatstein (2001), dolomitic stones have not found widespread use in atmospheric fluidized bed combustors because they are not particularly effective on a mass basis due to the inability of MgO to react with SO_2.

However, the sulphation reaction is far from ideal. Typically, only a conversion of 30–40% of CaO is obtained. This relatively low utilization of limestone is one of the major limitations of the technology (Anthony and Granatstein, 2001). The presence of SO_2 affects limestone particle size because it generates a hard sulphate shell around the unreacted CaO core of the particle, which reduces its fragmentation (Scala *et al*., 2011). Therefore, substantial changes in the sorbents' particle size distribution can be achieved from particle attrition and fragmentation

*To whom correspondence should be addressed

in fluidized bed combustors (Montanagro *et al*., 2010).

Because the molar volume of $CaSO_4$ is 52.2 cm^3/mol, which is greater than that of $CaCO_3$ (36.9 cm^3/mol), and no particle expansion occurs, the possible maximum practical conversion is low. Considering the bed temperature, it has been well established that the most favorable temperature for the sulphation reaction is located in the range of 800-850 °C, and the retention falls sharply as temperature increases (Yates, 1983). Moreover, excess air increases the changes in the gas composition in which the sorbent sulphates and the partial pressure of oxygen are increased; consequently, the partial pressure of CO_2 is reduced (Ulerich *et al*., 1980).

Different aspects of the desulphurization mechanism have already been investigated and will be briefly discussed. Lyngfelt and Leckner (1989) investigated the SO_2 conversion relationship with process conditions, especially temperature. The oxygen concentration was considered in Collar's (2001) analysis, who evaluated pore structures in the reactivity of different limestones. It was observed that with an increase in the O_2 concentration, the desulphurization reaction was worse due to the additional SO_3 in the reaction. Tarelho *et al*. (2005) studied the influence of operational parameters for fluidized bed desulphurization. A constant Ca/S molar ratio of 3.5 was used. Furthermore, excess air values of 10, 25 and 50% were applied.

Hlincik and Buryan (2013) reported that limestones with lower CaO content can provide a better desulphurization capacity. This result occurs because the desulphurization reactions of the combustion gases are significantly negatively affected by the reaction of CaO with the ballast oxides of ash and limestone.

The reaction kinetics were was studied by Irfan and Balci (2002). For temperatures of 850 °C and below, the reaction occurred with two mechanisms due to pore plugging and changes in the chemical composition of the solid. Bragança *et al*. (2003) studied the influence of limestone characteristics to determine the kinetic parameters of desulphurization using a batch fluidized bed reactor.

Anthony and Granadstein (2001) investigated the fragmentation of sorbent particles. Furthermore, Bragança (1996) used dolomitic and magnesium limestone for the desulphurization of different particle sizes. Scala *et al*. (2000) used a bench-scale fluidized bed reactor to investigate the attrition behavior of two different limestones during calcination and sulphation. After sulphation of the pre-calcined lime, the attrition rate for both types of limestones tested decreased dramatically until a new steady-state value was reached.

Furthermore, models for the description of the conversion mechanism have been evaluated. Suyadal *et al*. (2005) explored the SO_2 breakthrough curves in the presence of O_2, CO_2, and H_2O steam and tested one deactivation model description of these curves obtained in an integral fluidized bed reactor.

Additionally, and related to this study, due to the need for a minimum residence time of the calcinated particles, elutriation must be considered in the desulphurization process in fluidized bed systems. Elutriation is referred to the separation or removal of fines from a mixture, and it occurs to a lesser or greater extent at all freeboard heights. However, the solid carryover is strongly affected by gas velocity, and the fraction of fines in the bed is only slightly affected by changing the size of the coarse material and the minimum fluidization velocity (Kunii and Levenspiel, 1991).

Altindag *et al*. (2004) demonstrated that the freeboard sulphur-capture was enhanced significantly by recycling the elutriated sorbent particles. A limestone with 93.21 wt. % $CaCO_3$ was used. In runs without flue gas recycling, a significant majority of the sulphur retention occured in the bed section. By introducing flue gas recycling, freeboard sulphur capture increased from 3.5% to 19.5%. This result occurred because, for fuels rich in volatile matter and combustible sulphur content, such as the ones used in this study, freeboard sulphur capture is enhanced significantly with recycling because the sulphur release to the freeboard is significant.

Montanagro *et al*. (2010) investigated the influence of temperature on the attrition of two limestones during desulphurization in a fluidized bed reactor. The experimental procedure was conducted at 900 °C with the goal of assessing the extent of the primary fragmentation. Furthermore, results were compared with those obtained at 850 °C for the same reactor. The fluidized bed desulphurization experiments were conducted using a synthetic gas with an SO_2-O_2-N_2 mixture of 1800 ppmv-8.5%-N_2 balance. A temperature increase resulted in a larger amount of elutriation. The elutriation occurred on a time scale comparable with the sulphation. Therefore, after a harder sulphate shell is formed around the limestone particles, the attrition process dominates. Furthermore, in this report, the limestone particles are characterized by a rather limited propensity to yield elutriated fines as a result of surface wear. This issue should be considered in continuous industrial desulphurization runs, since such a limitation to yield elutriated fines tends to accumulate desulphurization

products in the bed and change bed properties after long time runs.

Thus, Huda *et al*. (2006) demonstrated the influence of four coal types on the *in situ* desulphurization process in a 71 MW Pressurized Fluidized Bed Combustor (PFBC) demonstration plant. Important information on the formation of the bed material was discussed. White and yellow particles were formed in the bed after the desulphurization tests. The white particles were calcium carbonate or calcium carbonate coated with calcium sulphate while the yellow particles were calcium carbonate coated with calcium sulphate and Ca–aluminosilicate. Moreover, the $CaSO_4$ particles formed agglomerate. Thus, fly ash particles could be distinguished from one another through their morphologies.

Scala *et al*. (2011) studied the primary fragmentation of two limestones in a 1-meter-height batch scale fluidized bed under air combustion and oxyfuel combustion. Synthetic gases were used to provide the atmospheres. Two types of limestone were used: $CaCO_3$ over 96% and $CaCO_3$ over 99%. Additionally, the limestone type was determined to be a more important variable with respect to the fragmentation tendency. The particle size, bed temperature, and simultaneous occurrence of the sulphation reaction were found to have an insignificant influence on the limestone primary fragmentation under either atmosphere. Again, the tendency of changes in the elutriation mechanism is one important result when controlling fragmentation.

However, according to Montanagro *et al*. (2010), an investigation of the effect of bed temperature on the limestone attrition and fragmentation phenomena, as well as their connection with the sulphation behavior and microstructural properties, is still lacking and appears to be of great practical interest.

Scala *et al*. (2013) tested the fluidized bed desulphurization performance of lime particles obtained using a limestone slow calcination pre-treatment technique compared to the untreated material. Furthermore, the fragmentation and attrition processes were investigated. An externally heated stainless steel atmospheric bubbling fluidized bed reactor 40 mm in diameter and 1 m in height was used for the experiments. The pre-treatment technique appeared to induce a high mechanical strength in the sorbent particles (as opposed to the fragile lime generated after typical rapid fluidized bed calcination).

Thus, although this technology is regarded as a mature technology for *in situ* desulphurization, its dependence on local stone properties and interactions between the local stone/coal properties and the fluidization conditions may require further research (Altindag *et al*., 2004). Consequently, the use of coals from different regions is an aspect to be considered when studying desulphurization, especially Brazilian coals, which have poor data on fluidized bed combustion and desulphurization.

The primary objective of this study is to obtain fluidized bed operating parameters in a bubbling fluidized pilot plant for SO_2 conversion using an *in situ* dolomite feed. Different runs analyzed the fluid dynamic characteristics for two southern Brazilian coals, and the superficial velocity, flue gas recycling, elutriation behavior and stoichiometric analysis were investigated. Results may lead to the development of a fluidized bed desulphurization of Brazilian coals.

MATERIALS AND METHODS

Materials

Table 1 presents ultimate and proximate analysis of the coals used as well as the low heating value (LHV), and Table 2 presents the dolomite characterization. All of the materials from Tables 1 and 2 originate from the southern region of Brazil. Coal A and Coal B are from two different Brazilian federative states, Rio Grande do Sul and Santa Catarina, respectively.

Table 1: Characterization of the coal used on a dry basis.

Coal	A	B
VM (%)	20.70	12.29
C_{fixed} (%)	25.13	37.52
H_2O (%)	8.53	10.02
$C_{d.b.}$ (%)	39.25	40.66
$H_{d.b.}$ (%)	3.04	2.86
$S_{d.b.}$ (%)	1.45	1.90
$N_{d.b.}$ (%)	0.69	1.30
$O_{d.b}$ (%)	5.64	8.66
$Ash_{d.b.}$ (%)	49.93	44.63
LHV (MJ/kg)	15.978	15.697
d_p (μm)	133.4	159.5

d.b.: dry basis

Table 2: Dolomite characterization.

CaO (%)	24.5
SiO_2 (%)	23.8
Fe_2O_3 (%)	1.5
Al_2O_3 (%)	2.4
MgO (%)	20.0
Na_2O (%)	0.010
K_2O (%)	2.1
TiO_2 (%)	0.15
Non-burned C (%)	28.0
d_p (μm)	142.2
ρ_s (kg/m^3)	2607

Pilot Plant

Figure 1 presents a flowchart of the 0.25 MWth pilot plant used for performing the combustion runs. As indicated in the figure, solid fuels from the silos (1) and (3), with rates controlled by screws (2) and (5), are injected by gravity into the furnace (6) where combustion occurs. The generated gases flow into a material refractory cyclone (7), which allows a greater residence time for the gases at an appropriate temperature for the post-combustion chamber (9). The gases exit towards a heat exchanger (10), which pre-heats the air that enters into the bubbling fluidized bed. After the temperature reduction occurs in the heat exchanger, the gases are conducted through another cyclone (12). In the sequence, if air combustion occurs, gases are released by the chimney. If oxyfuel combustion occurs (not applied in this study), the air entrance is closed, the recycling valve is opened, the chimney is partially closed and part of the gas is recirculated. A forced draught fan (14) is applied to provide energy for the gases. Points P1, P2 and P3 represent the pressure control locations within the system. The bed is rectangular, composed of sand, with a width of 27 cm and a length of 97 cm. The freeboard height is 2.0 m. Bed characteristics are provided in Table 3. A gas distributor is constructed using parallel tubes with holes disposed along its length.

Table 3: Bed characteristics.

ρ_s (kg/m^3)	2466
ρ_{bulk} (kg/m^3)	1544
d_p (µm)	725
U_{mf} (m/s)	0.20
Height (m)	0.4

It should be noted that such bed characteristics concern the sand before combustion runs. After coal feed in the furnace, the bed tends to change mean particle diameter and density due to ash accumulation.

Flue gases analysis was performed by sampling at point P2 and using a HORIBA PG 250 equipment for a continuous analysis of the combustion gases. The total mass ash generation was calculated using the ash content for each coal and the fuel feed in kg/h. Mass ash collected by Cyclone #1 was taken to Silo #1 for each run and determined in kg/h. CaO content was determined using X-Ray Fluorescence (XRF) analysis for each ash type. Bed inlet and outlet temperatures, T04 and T05, respectively, were determined continuously using thermocouples.

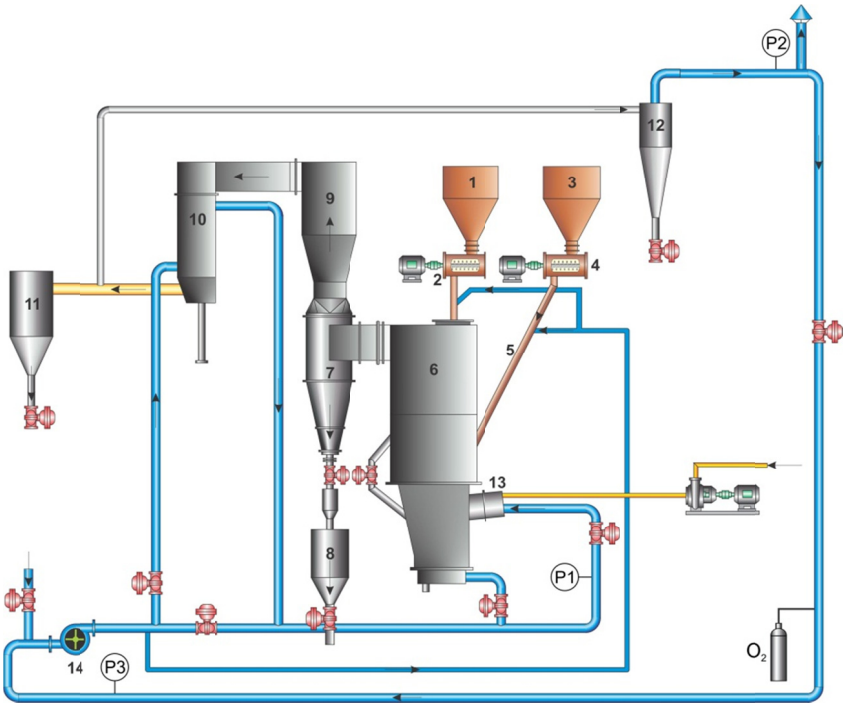

Figure 1: Pilot plant flowchart: (1) Dolomite silo; (2) Dolomite screw; (3) Coal silo; (4) Coal Screw; (5) Coal feed; (6) Reactor; (7) Cyclone #1; (8) Silo #1; (9) Post combustion chamber; (10) Heat exchanger; (11) Cyclone #2; (12) Chimney 2; (13) Heater; and (14) Forced draught fan.

Experimental Procedure

For the combustion runs, heating the bed began with an auxiliary fuel, ethanol, in the plant heater (13) until the bed reached 600-650 °C, which is when coal was added and the auxiliary fuel was not fed anymore. Fuel and air are adjusted to reach and stabilize the bed temperature at 850 ± 15 °C, when the steady-state condition was considered, which is controlled by two thermocouples located in the bed inlet, T04, and the bed outlet, T05. For each coal feed, after stabilizing the bed temperature, dolomite is added based on the applicable Ca/S relation.

For gas recycling, in order to provide a controlled transition, the following procedure was developed after reaching the steady-state condition on combustion:

I. 100% recycling gas valve open (valve gas recycling is located after the chimney);
II. Partial chimney closing via damper control; and
III. Progressive recycling valve closed to maintain positive pressure on point P2 of Figure 1.

Recycled gases were injected into the reactor entrance in the same air duct and passed through the draught fan (14). For the gas air mass flow rate control, to maintain the same conditions as applied to the air combustion without recycling with the U_s value, one valve located after the forced draught fan (Figure 1) was used to control the flow rate.

It is important to maintain a positive pressure until point P2 to prevent air leakage in the section reactor-P2 as gas sampling is performed in this section. The bubbling fluidization condition is controlled by the pressure drop, dP, in the bed, which must be maintained between 4413-5197 Pa, and temperatures T04 and T05, that cannot present a difference higher than 5 °C between bed inlet and outlet. Furthermore, the fluidization conditions can be continuously visualized through one observation point located above the reactor.

Stoichiometric Analysis

For the desulphurization reactions from the dolomite calcination, CaO and SO_2 are converted to $CaSO_4$ as described by Reactions 1 and 2. (Yates, 1983; Anthony and Granatstein, 2001).

$$CaO + SO_2 \rightarrow CaSO_3 \quad (1)$$

$$CaSO_3 + 1/2O_2 \rightarrow CaSO_4 \quad (2)$$

However, as also described by other authors, the desulphurization mechanism can be represented as the sum of Reactions 1 and 2, as expressed by Reaction 3 (Suyadal *et al*., 2005).

$$CaO + SO_2 + 1/2O_2 \rightarrow CaSO_4 \quad (3)$$

Average SO_2 Conversion Rate

Equation (4) expresses the rate of the SO_2 conversion, ξ, by taking its input and output and considering the reactor as the volume control.

$$\xi = \frac{n_{iSO2} - n_{oSO2}}{\upsilon_{SO2}} \quad (4)$$

where
n_{iSO2} = number of moles of SO_2 into the system;
n_{oSO2} = number of moles of SO_2 out of the system;
and
υ_{SO2} = SO_2 stoichiometric coefficient.
SO_2 was considered to be reacting based on Equation (3).

Desulphurization Efficiency

The desulphurization efficiency, η, can be obtained from Equation (5) as follows:

$$\eta(\%) = \frac{n_{iSO2} - n_{oSO2}}{n_{iSO2}} x100 \quad (5)$$

Reactants Consumption

Himmenblau and Riggs (2006) defined yield as the quantity of desirable product, $CaSO_4$, divided by the fed quantity of the reactant, CaO and SO_2. Here, the yield is considered as the $CaSO_4$ molar formation and is related to the molar quantity of reactant consumed, as $CaSO_4$/moles SO_2 feed and moles $CaSO_4$/ moles CaO feed.

Elutriation

Elutriation is considered as representing the wt.% of non-reacted CaO particles and ash particles carried out of the system during steady state conditions, as expressed by Equations (6) and (7). The CaO and ash particles were collected in Cyclone #1 of Figure 1.

$$\%\ \text{CaO Elutriated} = \frac{\text{mass}_{CaO}\ \text{elutriated}}{\text{mass}_{CaO}\ \text{fed into the bed}} \quad (6)$$

$$\%\ \text{Ash Elutriated} = \frac{\text{mass}_{Ash}\ \text{elutriated}}{\text{mass}_{Ash}\ \text{fed into the bed}} \quad (7)$$

Because the exiting CaO particles are supposed to be related to its residence time and, consequently, to its conversion, this component was selected to be considered in the elutriation analysis.

RESULTS AND DISCUSSION

The steady state conditions to obtain desulphurization data were considered to occur after the SO_2 concentration of the flue gases and the bed temperatures, T04 and T05, were stabilized. The bubbling fluidization conditions were experimentally confirmed by controlling the bed temperatures and the bed pressure drop, which must indicate, for the bed properties and the height used – 0.4 m, values between 4413 and 5197 Pa. Moreover, the fluidization and reaction conditions can be continuously controlled by visualization from the freeboard region.

Combustion, Desulphurization and Ash Composition Results

The results from the combustion of the coals used are presented in Table 4. For each coal, two conditions were taken by applying two different superficial velocities (U_s): 0.38 m/s and 0.46 m/s. P1 refers to the pressure in the reactor entrance and is higher for higher applied U_s, and ΔP is the pressure drop between the bed entrance and the exit.

Table 4: Air combustion runs.

Coal	A		B	
Condition	**A1**	**A2**	**B1**	**B2**
Air/Fuel Ratio	6.5	8.7	8.0	9.1
Air excess	75%	82%	65%	86%
U_s (m/s)	0.38	0.46	0.38	0.46
T05 (°C)	860	855	860	870
T04 (°C)	859	856	855	865
ΔP (Pa)	4884	4756	5394	5148
P1 (Pa)	7698	9159	7178	9120
P_f (Pa)	196	245	196	255
t_r (s)	0.76	0.49	0.61	0.60
FLUE GASES				
CO (ppm)	112	120	75	108
SO_2 (mg/Nm^3), 6% O_2	3350.1	3276.2	3861.8	4222.8

When using Coal B, and compared with Coal A, higher air/fuel ratios had to be applied to maintain the temperatures between 850 °C and 870 °C. Additionally, as a consequence of the latter, a higher O_2 % was maintained in the flue gases to achieve the same temperatures in the bed.

Bed material was the same in the Coal A and Coal B runs. Therefore, the differences between ΔP were the result of ash accumulation during the runs for maintaining the bubbling fluidization. It is important to highlight the values of pressure P1 for U_s = 0.38 m/s and U_s = 0.46 m/s. This parameter expresses the combustion air pressure in the reactor entrance, which is one of the most important process parameters related to solid elutriation out of the bed and the reactor.

According to Kunii and Levenspiel (1991), two dimensionless parameters, u^* and d_p^*, the dimensionless gas velocity and dimensionless particle size, respectively, can be introduced to map the fluidization regime. These parameters are defined as follows:

$$u^* = u\left[\frac{\rho_g^2}{\mu\left(\rho_s - \rho_g\right)g}\right]^{1/3} \tag{8}$$

$$d_p^* = d_p\left[\frac{\rho_g\left(\rho_s - \rho_g\right)g}{\mu^2}\right]^{1/3} \tag{9}$$

where "u" is gas velocity, "g" is the gravity, "ρ_g" is gas density, "ρ_s" is solid density and μ is gas viscosity.

In this way, Figure 2 shows the fluidization conditions according to the diagram for general flow condition presented by Kunii and Levenspiel (1991). As seen on Figure 2, all combustion conditions from Table 4 can be found in bubbling fluidized beds.

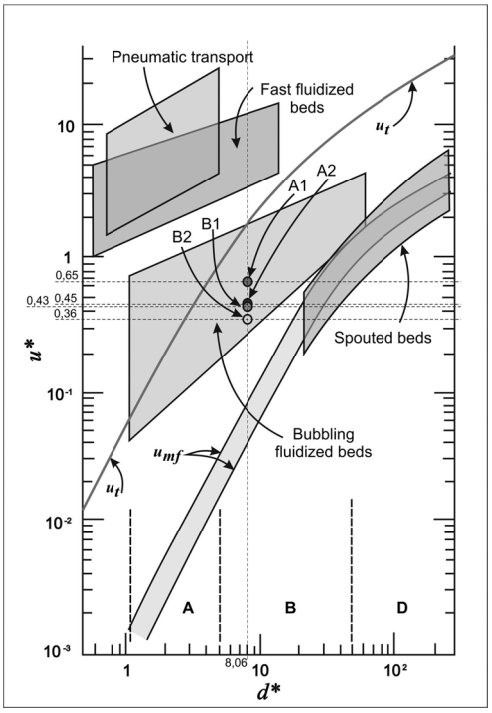

Figure 2: Fluidization mapping for Conditions A1, A2, B1 and B3. Adapted from Kunii and Levenspiel (1991), with permission.

Dimensionless particle diameter does not change because it is strongly affected by bed particle diameter, which was considered to be 530 μm from measurement due to the presence of coal ashes, differently from the previous bed diameter shown in Table 3. That bed diameter considered the bed being composed only of sand before coal ash accumulation.

Desulphurization Runs

After stabilizing air combustion conditions on each run, dolomite was fed in different conditions for the desulphurization runs. Upon introducing dolomite, the bed temperature decreased. However, the temperature rapidly recuperated. The dolomite feed was adjusted based on the coal feed and coal sulphur content for the required Ca/S molar ratio. After approximately 30 minutes for each condition, it was observed that the SO_2 concentration in the flue gases could achieve stabilization. Table 5 presents the different conditions applied for the desulphurization runs and the different coals tested. For each coal, two superficial velocities – U_s – were applied, 0.38 m/s and 0.46 m/s. Additionally, for each U_s value, three Ca/S molar ratios were used: 1.5, 2.0 and 2.5.

Table 5: Desulphurization conditions.

Condition	A3	A4	A5	A6	A7	A8
U_s (m/s)	U_s = 0.38 m/s			U_s = 0.46 m/s		
Ca/S Molar Ratio	1.5	2.0	2.5	1.5	2.0	2.5
Dolomite (kg/h)	3.8	5.0	6.3	6.0	8.1	10.0
SO_2 (mg/Nm^3), 6% O_2	1591.3	1256.3	988.3	1811.7	1779.0	1281.0
SO_2 (g/10^{6}kcal	2754.2	2174.4	1710.5	3496.7	3433.6	2472.4
Condition	**B3**	**B4**	**B5**	**B6**	**B7**	**B8**
U_s (m/s)	U_s = 0.38 m/s			U_s = 0.46 m/s		
Ca/S Molar Ratio	1.5	2.0	2.5	1.5	2.0	2.5
Dolomite (kg/h)	6.3	8.4	10.5	6.8	9.1	11.4
SO_2 (mg/Nm^3), 6% O_2	2432.9	1861.4	1564.0	3006.6	2195.8	2221.2
SO_2 (g/10^{6}kcal)	4883.5	3736.4	3139.4	6404.3	4677.2	4731.3

Table 5 also presents SO_2 concentration in mg/Nm^3 after desulphurization runs for 6% O_2 in the flue gases. From such results, SO_2 emissions in g/10^{6}kcal are presented for each desulphurization run, which are the units in the Brazilian Regulation CONAMA 08/1990. This regulation establishes SO_2 emission limits for coal power plants between 2000 and 5000 g SO_2/10^6 kcal. By comparing values presented in Table 5 with SO_2 range limits, it is possible to realize the necessity of a CONAMA 08/1990 update, as bubbling fluidized bed *in situ* desulphurization has the main objective of reducing as much as possible the SO_2 concentration in order to reduce Flue Gas Desulphurization equipment requirements.

Figure 3 presents the SO_2 conversion results applied to Coal A and Coal B for U_s = 0.38 m/s and U_s = 0.46 m/s. When comparing the different U_s values applied, a general trend for better conversions from higher residence times with smaller U_s values is observed. Additionally, when comparing Coal A and Coal B, better results were achieved for the SO_2 conversion with Coal A.

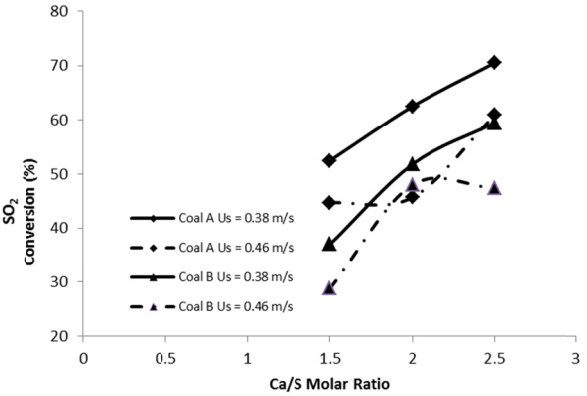

Figure 3: SO_2 conversion for Coal A and Coal B.

Furthermore, it should be noted that the SO_2 conversion depends on several factors, such as sorbent properties, fluid dynamic conditions and coal characteristics. According to Bragança *et al*. (2003), magnesium limestone is more efficient for short particle residence times. However, the sulphation reaction rate depends on the SO_2 concentration around the particles and the mean residence time of the particles in the bed. A higher fluidization velocity than the minimum velocity for the limestone provides lower desulphurization efficiencies.

Generally, for lower fluidization velocities, a higher SO_2 conversion was achieved for both coal types, which occurs due to the resulting higher residence times of the particles within the bed. Here, a direct fluid dynamic influence can be assessed. By analyzing the influences of the coal characteristics due to the sulphur content, as will be better discussed in the stoichiometric analysis, even though Coal B provided a lower SO_2 conversion, the sulphation reaction rate was higher. This result indicates that to provide a desulphurization conversion similar to that

of Coal A, the Ca/S relation must be increased to decrease the SO_2 concentration around the sorbent particles.

The influence of the SO_2 concentration around the sorbent particles on the conversion can be confirmed by XRF analysis of the non-desulphurized ashes, A1 and B1, as indicated in Table 6. The alkaline and alkaline earth components of the coal ashes influence the desulphurization behavior by providing self-desulphurization (Cheng *et al*., 2003). Table 6 indicates that the alkaline components of Coal B are higher compared to those for Coal A, especially for CaO. By considering that the dolomite characteristics were the same for both coals and taking the same superficial velocity, the SO_2 concentration of the flue gases is confirmed to provide higher influence on conversion than the coal ash characteristics.

By using mean diameter and the density of dolomite, as expressed in Table 2, the terminal velocity can be calculated as 0.62 m/s. If we compare this terminal velocity with the superficial velocities applied in the experiments, the superficial velocities are 61.3% and 74.2% of the dolomite terminal velocity for U_s = 0.38 and U_s = 0.46 m/s, respectively. Consequently, since the dolomite is fed just above the bed, the particles are prone to reach the bed and start the fragmentation and calcination process in the bubbling bed. Moreover, it should be noted that a visual observation of the bed after the desulphurization runs indicated a concentration of white and yellow desulphurization product particles, which confirmed the high dolomite and Ca-containing products within the bed as a result of the change in its properties after long runs and will be discussed later. Thus, in industrial plants, this result indicates the necessity of controlling the changes in bed properties after long runs for bed reposition.

Table 6: XRF analysis of Coal A1 and Coal B1 ashes.

Condition	A1	B1
CaO (%)	2.2	6.91
SiO_2 (%)	592	58.0
Fe_2O_3 (%)	8.51	5.64
Al_2O_3 (%)	23.6	19.0
MgO (%)	0.70	3.50
Na_2O (%)	0.15	0.20
K_2O (%)	1.93	2.68
TiO_2 (%)	0.85	0.78
SO_3 (%)	2.18	2.57
Non-burned C (%)	0.56	0.61

However, an increase in the diameter of the dolomite is not necessary to increase the terminal velocity because it would increase the mass transfer resistance and decrease the SO_2 conversion, as well as increase the size and concentration of the desulphurization products that accumulate in the bed.

Furthermore, as seen in the XRF analysis in Table 6, self-desulphurization had already occurred without the sorbent feed due to the $CaSO_4$ formation because SO_3 appears significantly together with CaO. This result occurs because the coal ashes present CaO in their composition that can react with SO_2. However, this self-desulphurization mechanism cannot only be predicted by the Ca in the ash composition due to the presence of other alkaline elements that are able to promote self-desulphurization (Cheng *et al*., 2003).

Desulphurization with Gas Recycling

The possibility of increasing the SO_2 conversion with flue gas recycling was analyzed. The same conditions applied for the desulphurization runs using U_s = 0.38 m/s, and a Ca/S molar ratio of 2.0 was considered in the desulphurization with recycled gas. Table 7 presents the conditions and results obtained from these runs. To maintain the same superficial velocity as in condition B4, the total air plus gas flow rate was controlled by one valve located after both fluxes, i.e., just after the forced draught fan (Figure 1).

Table 7: Desulphurization results with gas recycling runs.

Coal	B
U_s (m/s)	0.38
Ca/S Molar Ratio	2.0
Dolomite (kg/h)	8.4
SO_2 Conversion (%)	86.1
SO_2 (mg/Nm^3), 6% O_2	536.8
SO_2 (g/10^6kcal)	1143.4
Gas recycling (%)	54.6

Table 7 indicates that the SO_2 conversion can be strongly increased from 48.0% to 86.1% when recycling part of the flue gases. Consequently, some elutriated and non-converted CaO particles are able to return to the reactor to react with SO_2. Here, the percentage of gases recycled is referred to as the wt. % of gases returning to the fluidized bed from the total flue gas flow. In this way SO_2 emission, according to Brazilian regulations, can be reduced to 1143.4 g/10^6 kcal, far lower than the ones obtained in Table 5.

Furthermore, Altindag *et al*. (2004) applied fine recycling for lignite desulphurization. The introduction of recycling increased the sulphur retention efficiency from 68.5% to 81.1% as a result of the increased residence time of unreacted or partially

sulphated recycled fine limestone-particles. According to the authors, for fuels that are rich in volatile matter and combustible sulphur content, the freeboard sulphur capture and release to freeboard was significantly enhanced with recycling. These observations could be applied to Brazilian coal due to its low fixed carbon content and high volatile matter.

Stoichiometric Analysis

The desulphurization reactions considered the relation of 1 mol $CaSO_4$ per mol of SO_2 reacted as well as 1 mol $CaSO_4$ per mol of CaO reacted. Consequently, considering the results before, Table 8 presents the values for a $CaSO_4$ yield based on a SO_2 and CaO feed. Table 8 also provides an average SO_2 conversion rate for the number of moles of SO_2 consumed/hour.

From Table 8, a comparison can be made between the runs obtained from one type of coal and different U_s values, such as A4 x A7 and B4 x B7. It can also be made for the same U_s and different coals, such as A4 x B4 and A7 x B7.

If we consider the reactant consumption, as expressed by moles $CaSO_4$/moles SO_2 feed and moles $CaSO_4$/moles CaO feed, few differences can be observed when comparing A4 x A7 and B4 x B7 conditions. For the same type of coal, the number of moles formed per SO_2 and CaO moles consumed were higher for the lower U_s. Here, it can be observed that reactants are consumed better at a higher residence time, as expected.

Table 8: Stoichiometric analysis of desulphurization runs for Ca/S = 2.0.

Condition	moles $CaSO_4$/moles SO_2 feed	moles $CaSO_4$/moles CaO feed	ξ (n°moles/h)
A4	0.625	0.333	-7.29
B4	0.518	0.322	-10.35
A7	0.457	0.225	-7.98
B7	0.480	0.273	-8.79

When comparing conditions A4 x B4 and A7 x B7, i.e., for the same fluid dynamic conditions but different coals, there are some few points that should be considered. Different values are observed for the average SO_2 conversion rate. Even with lower SO_2 conversion values for Coal B under conditions A4 x B4 and a similar conversion under conditions A7 x B7, Coal B presented higher conversion rate values; SO_2 conversion can be observed in Figure 3. This behavior is a result of the S wt.%, which is higher for Coal B and responsible for a higher reaction rate. Moreover, for the same coal, the fluid dynamic conditions indicated an influence. For U_s = 0.38 m/s, the reaction extent was 10.35 moles SO_2/h under condition B4 and – 8.79 moles SO_2/h under condition B7. This decrease in the conversion rate with Coal B, which was not observed for Coal A, could explain the behavior observed in Figure 3 for this coal with U_s = 0.46 m/s.

Ash Characterization

During coal combustion, a part of the total sulphur in the coal will be retained as solid compounds in the ash. This signifies that the coal ash has a sulphur-retaining property, which makes a significant contribution to alleviating the problem of SO_2 emissions (Sheng *et al*., 2000). According to the same authors, most of the calcium in coal is active and capable of participating in sulphur-retention reactions during coal combustion. Additionally, the content of calcium in most coals is generally significantly higher compared to that of other basic elements. Therefore, variations in the Ca/S molar ratio in coal can markedly affect the percentage of sulphur retained.

The X Ray Diffraction (XRD) patterns for the two coal ashes studied are illustrated in Figures 4 and 5. Both figures indicate non-desulphurized ashes, a Ca/S molar ratio of 2.0 for U_s = 0.38 m/s and Ca/S molar ratio 2.0 for U_s = 0.46 m/s. For non-desulphurized coal ashes – A1 and B1 – the main phases are hematite (Fe_2O_3) and anhydrite ($CaSO_4$) instead of SiO_2 and silicates. For better phase representation, SiO_2, which is the main ash phase, and silicates are not identified in Figures 4 and 5. The main peaks of other phases are identified in the same figures.

Concerning SO_4^{2-} based compounds, most organic sulphur and pyrite in coal are oxidized and converted to SO_2 gas during the combustion in furnaces. A small part of the sulphur may be retained as solid compounds due to the contribution of alkaline components, such as CaO, MgO, Al_2O_3, K_2O and Na_2O in the coal ash. The desulphurization property of the coal ash during combustion is primarily affected by the boiler shape, flame temperature, residence time in the furnace, initial molar ratio of Ca/S and reaction activity of the alkaline components. It is difficult for sulphates of other minor elements, such as $MgSO_4$, $Al_2(SO_4)_3$, $Fe_2(SO_4)_3$, K_2SO_4 and Na_2SO_4, which are less thermally stable than $CaSO_4$, to act as sulphation products during the coal combustion at high temperatures (Cheng *et al*., 2003).

Muscovite ($KAl_2(AlSi_3O_{10})(OH)_2$) was the primary silicate identified in the Coal A and Coal B ashes.

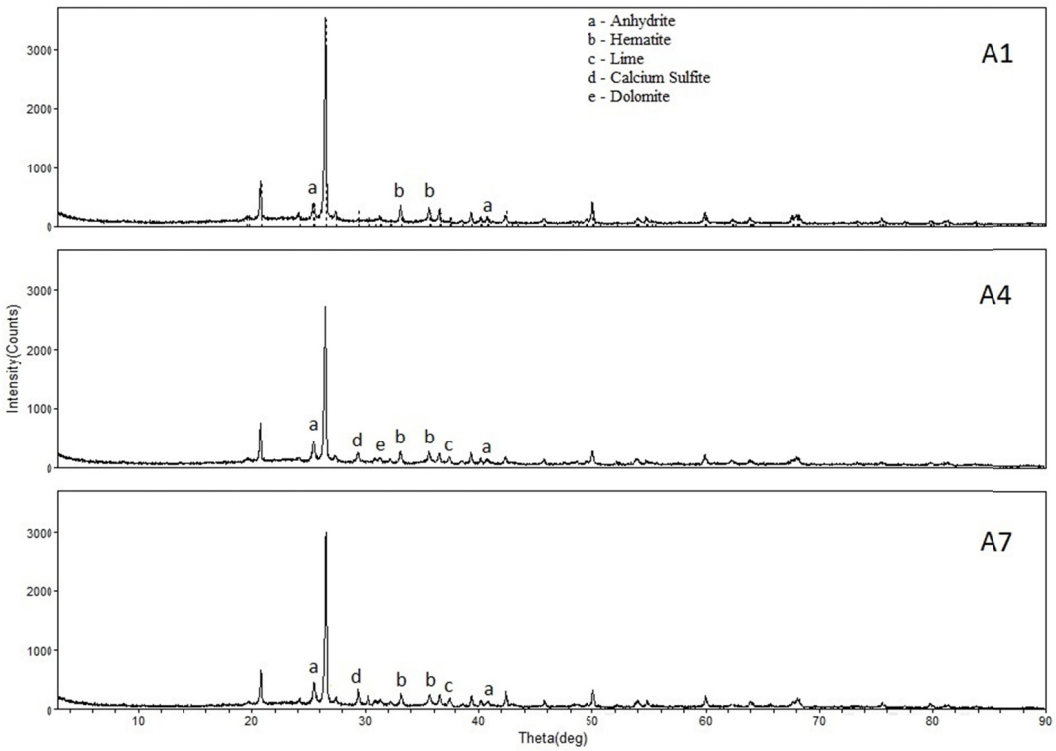

Figure 4: XRD patterns for Coal A ashes (A1) Without desulphurization; (A4) Ca/S 2.0, U_s = 0.38 m/s; and (A7) Ca/S 2.0, U_s = 0.46 m/s.

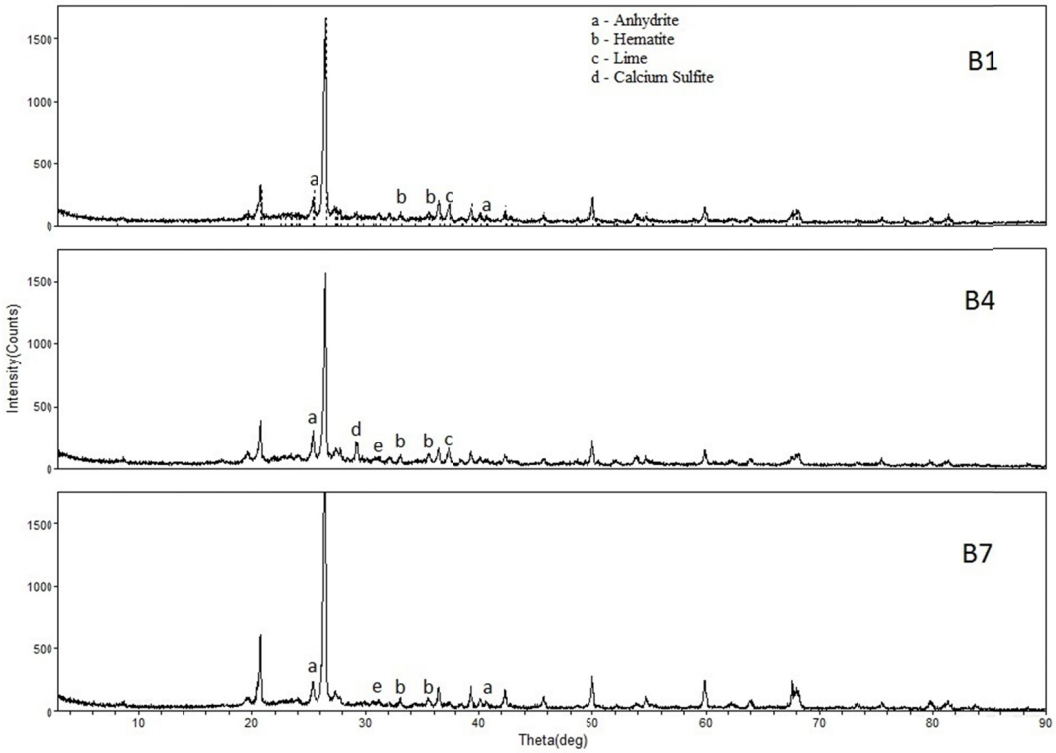

Figure 5: XRD patterns for Coal B ashes (B1) Without desulphurization; (B4) Ca/S 2.0, U_s = 0.36 m/s; and (B7) Ca/S 2.0 and U_s = 0.46 m/s.

A strong presence of hematite was observed in the Coal A ashes. By analyzing Figure 4, it is clear that differences exist between the ashes generated with and without desulphurization. The anhydrite peaks appear to be more intense after dolomite ($CaMg(CO_3)_2$) and lime (CaO) additions due to the desulphurization mechanism, as previously discussed.

Considering the hematite formation, according to Brady *et al*. (1994), the dominant reaction for FeS contained in coals can be written as follows:

$$FeS + CaCO_3 + 1/2O_2 \rightarrow Fe_2O_3 + CaSO_4 + CO_2 \quad (10)$$

The presence of calcium sulphite in conditions A4, A7 and B4 indicates that the desulphurization reactions did not have time to be completed. This may have occurred because, as soon as the gases exited the reactor, they were captured by Cyclone #1, and the reactor's temperature rapidly decreased.

The rate of formation of sulphur-containing solid components (sulphide, sulphite and sulphate) appears to be nearly independent of the presence of oxygen at temperatures below approximately 735 °C. At 830 °C, where calcium sulphite is unstable in the prevailing atmosphere, the rate of formation of sulphur-containing components is increased by the presence of oxygen (Dam-Johansen and Ostergaard, 1991). The same authors note that the formation of calcium sulphate from calcium oxide, sulphur dioxide and oxygen may occur through the formation of calcium sulphite and the subsequent disproportionation to calcium sulphate and calcium sulphide, oxidation to calcium sulphate, or through catalyzed or uncatalyzed oxidation of sulphur dioxide to sulphur trioxide and the subsequent reaction with calcium oxide. Calcium sulphide was not observed in all of the ashes, which suggested that the disproportionation of calcium sulphite may not have occurred. The XRD patterns suggest that the formation of $CaSO_3$ occurs first and is then followed by oxidation to $CaSO_4$, as indicated by Reactions 1 and 2.

Elutriation

The elutriation behavior of the ashes and the desulphurization products was analyzed. Consequently, conditions A4 and A7 were compared, because the Ca/S relation was the same for both conditions but the superficial velocities applied were different. The elutriation analysis had the primary objective of assessing the desulphurization products' partitioning behavior within the bed and Cyclone #1.

The XRF analysis of the ashes from conditions A4 and A7 are presented in Table 9. The goal was to consider the quantitative oxide analysis to serve as a basis for determining the CaO partitioning. Thus, Table 10 presents the mass collected and the ash mass flow within Cyclone #1 producing the ashes in Silo #1. Consequently, from the total ash generation, the wt. % ashes obtained in Silo #1 from the operation of Cyclone #1 can be determined. Furthermore, by obtaining the CaO feed from the dolomite and the non-desulphurized ashes, the wt. % CaO collected in Cyclone #1 was also determined in Table 10.

From Table 10, it can be seen that 60.5 wt.% of the ashes in condition A4 were obtained in Silo #1 and 55.4 wt.% from condition A7 were obtained in the same silo. The values for the wt. % CaO fed into the reactor (dolomite + non-desulphurized ashes), elutriated and collected by Cyclone #1 and stored in Silo #1 were not within the same range; for condition A4, 43.07 wt.% of the fed CaO was collected by cyclone #1 whereas 37.32 wt.% was collected by the same cyclone under condition A7.

From the first analysis, it can be seen that the elutriation and the collection of ashes and Ca-containing products do not present the same behavior.

Table 9: XRF for Coal A ashes.

Condition	A4	A7
CaO (%)	6.80	6.96
SiO_2 (%)	56.0	53.8
Fe_2O_3 (%)	7.03	7.23
Al_2O_3 (%)	19.5	21.5
MgO (%)	3.51	3.63
Na_2O (%)	0.20	0.14
K_2O (%)	1.72	1.57
TiO_2 (%)	0.79	0.83
SO_3 (%)	3.47	3.44

Table 10: Elutriation analysis of Coal A ashes and CaO obtained from Cyclone #1 under conditions A4 and A7.

Condition	A4	A7
Ashes from Silo 1 (kg)	1.94	2.98
% Ash Silo #1	60.5	55.4
% CaO Silo #1	43.07	37.32
Cyclone #1 collection rate (kg/h)	7.76	10.64

The typical tendency is that the elutriation of solids increases as U_s increases. However, it can be seen that the wt. % of CaO in Silo #1 was lower for condition A7 when a higher U_s value was applied. This result was distinctly different than expected.

Therefore, a hypothesis can be developed that such values for Ca-containing solids collected in Silo #1 are the highest independent of the U_s value applied. This hypothesis is supported by the fact that the elutriated bed was seen in the ashes collected in Silo #1 from condition A7. In other words, it can be stated that, even upon increasing the U_s value and the elutriating bed fines, the Ca-containing products, or desulphurization products collected by Cyclone #1 did not increase. Moreover, a visual observation of the bed behavior during the runs under such conditions showed slugging fluidization behavior.

Consequently, it can be asked whether the remainder ash and the CaO partitioning were more concentrated: (i) in the bed or (ii) by fragmentation, which could not be collected by Cyclone #1. Figure 6 presents the XRD patterns of the bed material after the Coal A desulphurization runs. The products from the dolomite addition for the *in situ* desulphurization can be observed in the figure. These results suggest that desulphurization products, if not collected by Cyclone #1, tend to be concentrated in the bed. Furthermore, this result helps to explain the lower CaO concentration in Silo #1 compared with the ashes, as indicated in Table 10, because the Ca-containing products tend to stay in the bed. From visual observation of the bed material after the Coal A runs, the presence of white and yellow materials with sizes larger than the bed sand could be observed. The bed material before the desulphurization runs was only composed of sand.

In fact, Scala *et al*. (2000) observed a decrease in the elutriation associated with the conversion progress due to the formation of desulphurization products in the bed. Furthermore, it should be noted that Montanagro *et al*. (2010) discovered that the attrition and fragmentation during calcination and sulphation in a bubbling bed operating at low gas superficial velocity were moderate to negligible for all the sorbents tested.

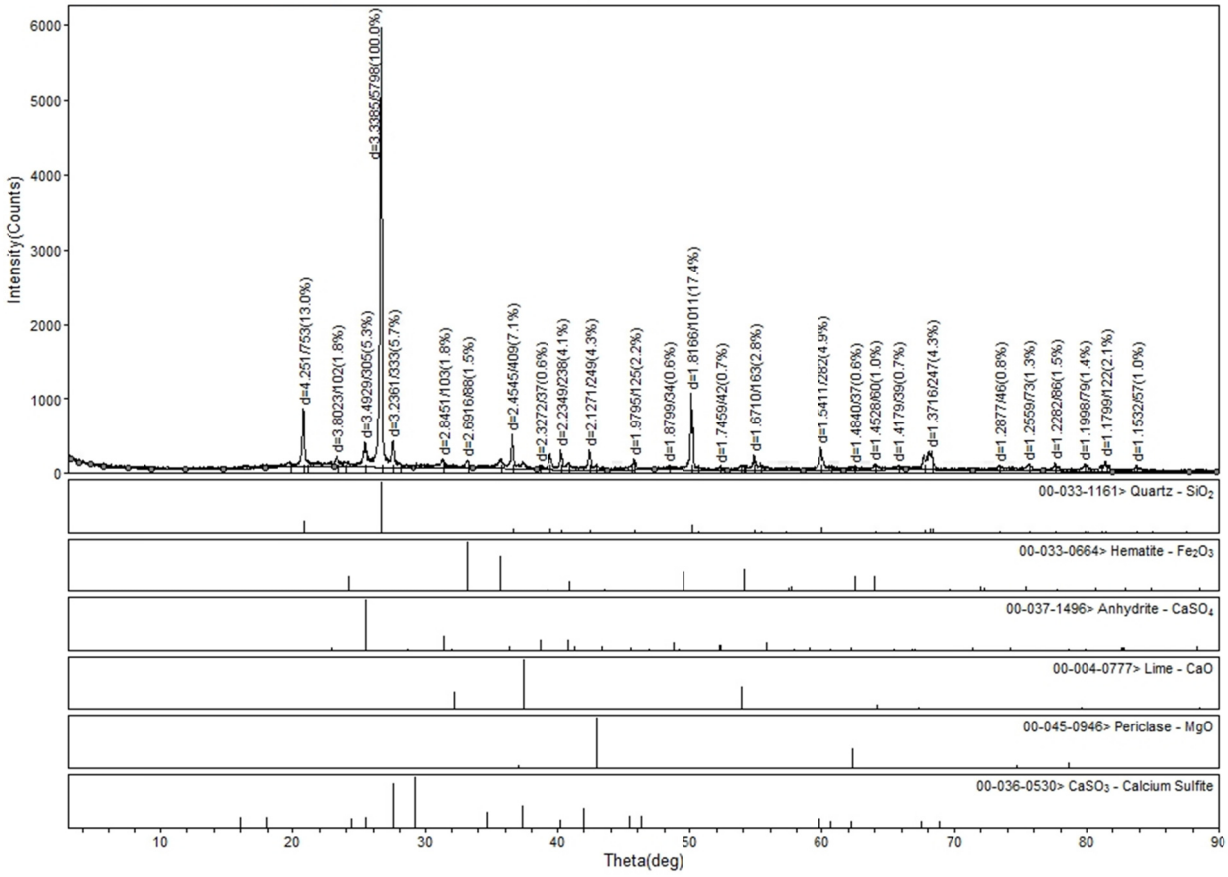

Figure 6: XRD patterns for the bed material after Coal A desulphurization runs.

Additionally, Huda *et al*. (2006) observed white and yellow bed materials larger than 2.0 mm after the *in situ* desulphurization. They noted that the yellow particles were $CaCO_3$ coated with $CaSO_4$ and Ca-aluminosilicate while the white particles were $CaCO_3$ or $CaCO_3$ coated with $CaSO_4$. Consequently, the authors defined the Ca/S molar ratio of the fine sorbent formed by attrition (< 200 μm), which was significantly lower than the total Ca/S molar ratio.

From the elutriation analysis, it can be noted that, for long dolomite desulphurization runs on the bubbling fluidized bed, there is a tendency of the bed properties to change for coal types similar to the Brazilian ones. It is important that this be controlled in industrial plants so that the fluidization quality is not affected.

CONCLUSIONS

After analyzing different aspects that involve *in situ* desulphurization in a bubbling fluidized pilot plant, some conclusions can be developed for the SO_2 conversion, ash characteristics and elutriation mechanisms.

Based on the stoichiometric analysis performed on the SO_2 conversion, i.e., a comparison of one coal under different fluid dynamics conditions, Coal B presented higher SO_2 conversion rates. This was the expected result for a higher S wt.% for this fuel. Additionally, better conversion was observed for lower U_s values; however, Coal B presented lower conversion rate values for SO_2 consumed per hour for U_s = 0.46 m/s.

The fluidization slugging behavior when applying a higher superficial velocity, U_s = 0.46 m/s, and a bed height of 0.4 m for 0.262 m^2, indicated a considerable decrease in the SO_2 conversion, which was most likely due to changes in the mass transfer mechanism. Together, the changes in the residence time must be considered to some extent. However, the residence time was not able to explain the SO_2 conversion because, for example, in the Coal B conditions, it showed the same value for both superficial velocities applied. Consequently, the fluidization condition with a mass transfer mechanism can be a better path for achieving the SO_2 conversion relations.

Mineralogical analyses for the ash characterization indicated the presence of $CaSO_4$ and $CaSO_3$ as desulphurization products. Because no CaS was observed in the ashes, it can be suggested that the mechanism for $CaSO_4$ formation occurs by the formation and oxidation of $CaSO_3$. This issue is important to be controlled when considering the use of ash. The formation of $CaSO_4$ instead of $CaSO_3$ is often preferred when considering the different structural uses of coal ashes.

The different fluid dynamic conditions applied clearly indicated a lower percentage of CaO in Cyclone #1 than the quantity fed compared with the same relation for the ashes fed into the reactor. This behavior was explained by the tendency of desulphurization products to accumulate in the bed during the use of dolomite. It was confirmed by visually detecting the desulphurization products as larger white particles in the bed. Again, it is an important issue to be considered in the continuous run of bubbling fluidized bed plants working with *in situ* desulphurization due to the strong tendency of changes in the bed properties. Consequently, some continuous bed control must be developed by an appropriate procedure. Moreover, property changes in long desulphurization runs are still an issue to be analyzed in future studies.

NOMENCLATURE

C_{fixed}	fixed carbon
d_p	particle diameter (μm)
d_p^*	dimensionless particle diameter
P_f	freeboard pressure (mmH_2O)
P	Pressure (mmH_2O)
T04	Inlet bed temperature (°C)
T05	Outlet bed temperature (°C)
t_r	residence time (s)
u	gas velocity (m/s)
U_{mf}	minimum fluidization velocity (m/s)
U_s	superficial velocity (m/s)
u^*	dimensionless gas velocity
VM	volatile matter
XRD	X-Ray Diffraction
XRF	X-Ray Fluorescence
ΔP	bed pressure variation (mmH_2O)

Greek Letters

ξ	Average SO_2 conversion rate (moles SO_2/h)
ρ_g	gas density (kg/m^3)
ρ_s	solid density (kg/m^3)
ρ_{bulk}	bulk density (kg/m^3)
μ	gas viscosity (kg/m.s)

ACKNOWLEDGEMENTS

We would like to thank National Council of Scientific and Technological Development – CNPq – from Brazil for the financial support and Foundation of Science and Technology of the State of Rio

Grande do Sul (CIENTEC/RS) for supplying the Campus' plants for the combustion tests.

REFERENCES

Altindag, H., Gogebakan, Y. and Selçuk, N., Sulphur capture for fluidized-bed combustion of high-sulphur lignite. Applied Energy, 79, 403 (2004).

Anthony, E. J. and Granatstein, D. L., Sulphation phenomena in fluidized combustion systems. Progress in Energy and Combustion Science, 27, 215 (2001).

Brady, M. E., Burnett, M. G., Galwey, A. K., Murray, O. and Sharkey, R., Aspects of the chemistry of calcium sulphate in coal ash. Fuel, 73, 39 (1994).

Bragança, S. R., Dessulphuração do Gás de Combustão do Carvão Candiota em Leito Fluidizado: Influência da Razão Molar Ca/S, Granulometria e Composição Química do Sorbente. Ph.D. Thesis, Universidade Federal do Rio Grande do Sul (1996). (In Portuguese).

Bragança, S. R., Jablonski, A., Castellan, J. L., Desulphurization kinetics of coal combustion gases. Brazilian Journal of Chemical Engineering, 26(2), 161-169 (2003).

Cheng, J., Zhou, J., Liu, J., Zhou, Z., Huang, Z., Cao, X., Zhao, X., Cen, K., Sulphur removal at high temperature during coal combustion in furnaces: A review. Progress in Energy and Combustion Science, 29, 381 (2003).

Collar, S. A. C., Influência da Estrutura de Poros e do Raio de Grão na Reatividade ao SO_2 de Calcinados de Calcários Gaúchos. Ph.D. Thesis, Universidade Federal do Rio Grande do Sul (2001). (In Portuguese).

CONAMA, (Conselho Nacional do Meio Ambiente), Regulation N°08 from 6-December-1990. Establishes emission standards for external combustion systems.

Dam-Johansen, K., Ostergaard, K., High-temperature between sulphur dioxide and limestone – IV. A discussion of chemical reaction mechanism and kinetics. Chemical Engineering Science, 46(3), 588 (1991).

Deer, W. A., Howie, R. A., Zusmann, J., An Introduction to the Rock Forming Minerals. Addison Wesley Longman Limited, London (1992).

Himmelblau, D. M., Riggs, J. B., Basic Principles and Calculations in Chemical Engineering. Pearson, New Jersey (2006).

Hlincik, T., Buryan, P., Evaluation of limestones for the purposes of desulphurization during the fluid combustion of brown coal. Fuel, 104, 208 (2013).

Huda, M., Mochida, I., Korai, Y., Misawa, N., The influences of coal type on in-bed desulphurization in a PFBC demonstration plant. Fuel, 85, 1913 (2006).

Irfan, A., Balci, S., Sulphation reaction between SO_2 and limestone: Application of deactivation model. Chemical Engineering and Processing, 41, 179 (2002).

Kunii, D., Levenspiel, O. Fluidization Engineering. Butterworth, Newton (1991).

Lyngfelt, A., Leckner, B., Sulphur capture in fluidized bed boilers: The effect of reductive decomposition of $CaSO_4$. The Chemical Engineering Journal, 40, 59 (1989).

Montangro, F., Salatino, P., Scala, F., The influence of temperature on limestone sulphation and attrition under fluidized bed combustion conditions. Experimental Thermal and Fluid Science, 34, 352 (2010).

Scala, F., Salatino, P., Boerefijn, R., Ghadiri, M., Attrition of sorbents during fluidized bed calcination and sulphation. Powder Technology, 107, 153 (2000).

Scala, F., Lupíañez, C., Salatino, P., Romeo, L. M., Díez, L. I., Primary fragmentation of limestone under oxy-firing. Fuel Processing Technology, 92, 1449 (2011).

Scala, F., Chirone, R., Meloni, P., Carcangiu, G., Manca, M., Mulas, G., Mulas, A., Fluidized bed desulphurization using lime obtained after slow calcination of limestone particles. Fuel, 114, 99 (2013).

Sheng, C., Xu, M., Zhang, J. and Xu, Y., Comparison of sulphur retention by coal ash in different types of combustors. Fuel Processing Technology, 64, 1 (2000).

Suyadal, Y., Erol, M. and Oguz, H., deactivation model for dry desulphurization of simulated flue gas with calcined limestone in a fluidized-bed reactor. Fuel, 84, 1705 (2005).

Tarelho, L. A. C, Matos, M. A. A. and Pereira, F. J. M. A., The influence of operational parameters on SO_2 removal by limestone during fluidized bed combustion. Fuel Processing Technology, 86, 1385 (2005).

Ulerich, N. H., Newby, R. A. and Keairns, D. L., A thermogravimetric study of the sulphation of limestone and dolomite – prediction of pressurized and atmospheric fluidized bed desulphurization. Thermochimica Acta, 36, 1 (1980).

Yates, J. G., Fundamentals of Fluidized-Bed Chemical Processes. Butterworths, Newton (1983).